Electronic Supplementary Material (ESI) for Nanoscale.
This journal is © The Royal Society of Chemistry 2014

Supplementary information

Probing planar defects in nanoparticle superlattices by 3D small-angle electron diffraction tomography and real space imaging

Arnaud Mayence, Dong Wang, German Salazar-Alvarez, Peter Oleynikov, Lennart Bergström*

1. TEM Bright-field images of faceted Pd nanoparticle superlattices

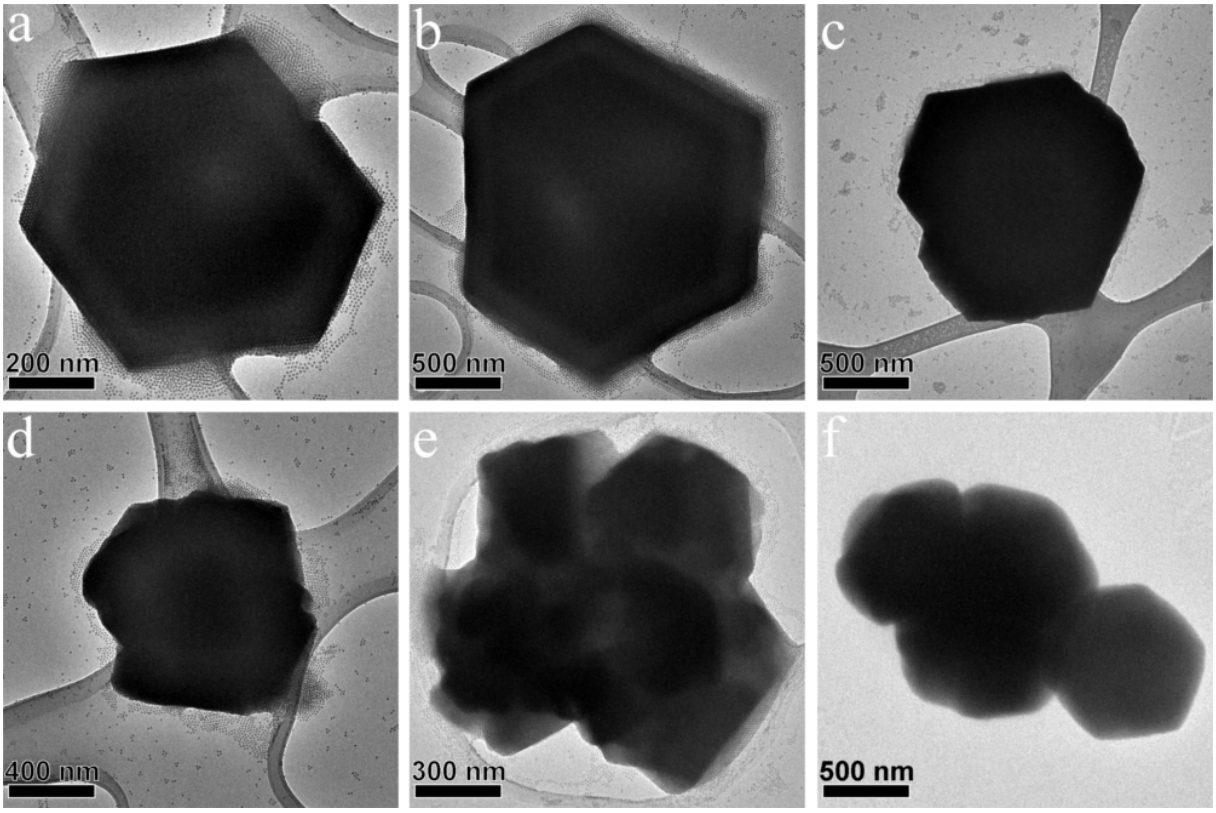

Figure S1. TEM bright-field images of facetted Pd nanoparticle superlattices, assembled during 72 hours, at different magnification. (a-b) hexagonal morphology. (c-d) deviating from a hexagonal morphology. (e-f) intergrowth.

2. Characterization of palladium nanoparticles

- Powder X-ray diffraction

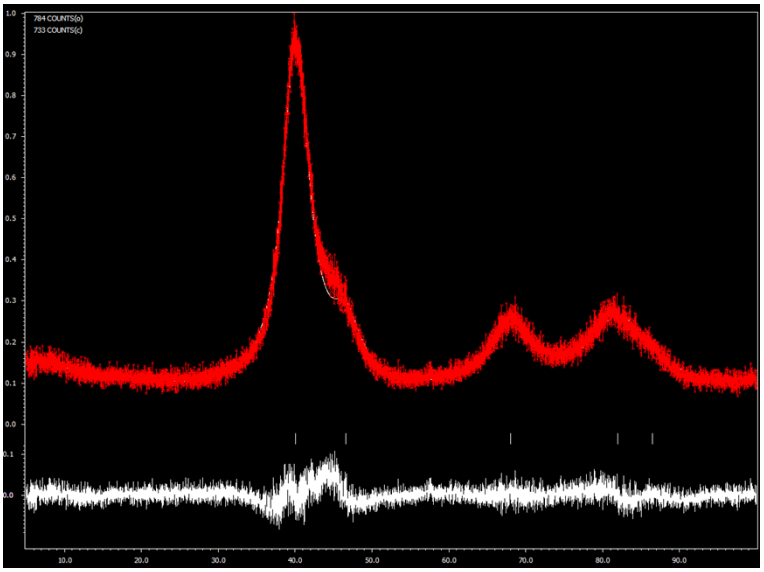

Figure S2. Powder X-ray diffraction pattern of palladium nanoparticles.

X-ray Powder diffraction (XRPD) was measured on a conventional in-house powder diffractometer using Cu $K_{\alpha 1}$ radiation. The refinement was performed using JANA2006 by profile fitting. A cubic lattice was found to be 3.9012(7) Å. The refined lattice parameter has further been used for calibration of the HRTEM images.

- HRTEM and size distribution assessment

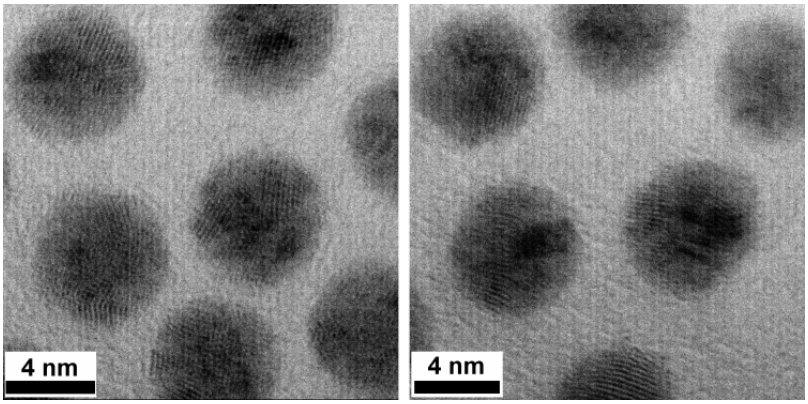

Figure S3. HRTEM images of palladium nanoparticles.

The size distribution (core of the nanoparticle) was estimated based on identified lattice planes from Pd nanoparticles over 150 nanoparticles. The size distribution diagram is shown in Figure S3. The mean particle diameter, d, and its standard deviation, σ, was determined by fitting the histogram with a normal distribution function:

$$f(x) = \frac{1}{\sigma\sqrt{2\pi}} exp\left[\frac{(x - d)^2}{2\sigma^2}\right]$$

The resulted diameter corresponds to, d = 6.1 ± 0.6 nm. The relative standard deviation corresponds to 9.3 % (calculated from the formula below):

$$\%RSD = \frac{\sigma}{d} \times 100$$

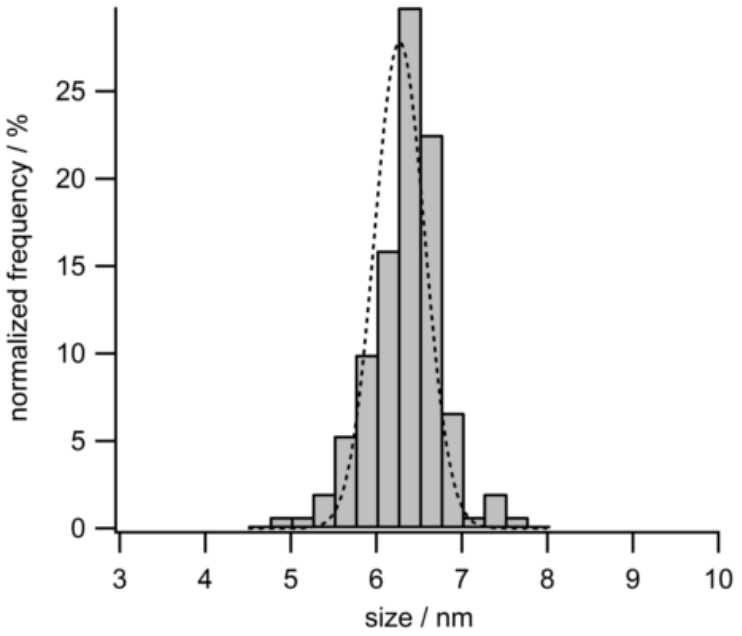

Figure S4. Histograms of the nanoparticles size distribution.

3. A comparison of experimental and simulated 3D reciprocal volume reconstruction

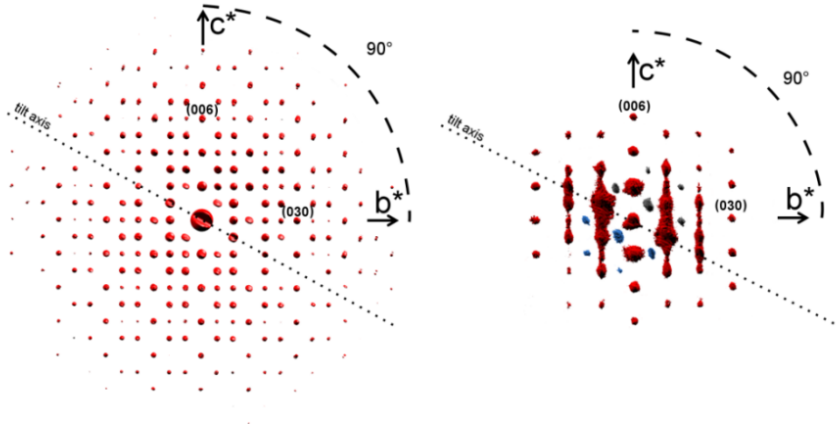

Figure S5. Three-dimensional reciprocal volume reconstruction. (right) Projection of experimental 3D data set along [100] and (left) projection of simulated 3D data set along [100] of an ideal hcp lattice (space group: $P6_3/mmc$).

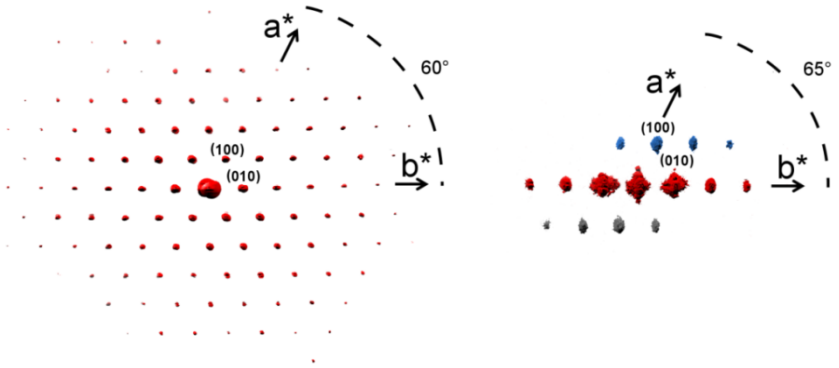

Figure S6. Three-dimensional reciprocal volume reconstruction. (right) Projection of experimental 3D data set along [001] and (left) projection of simulated 3D data set along [001] of an ideal hcp lattice (space group: $P6_3/mmc$).

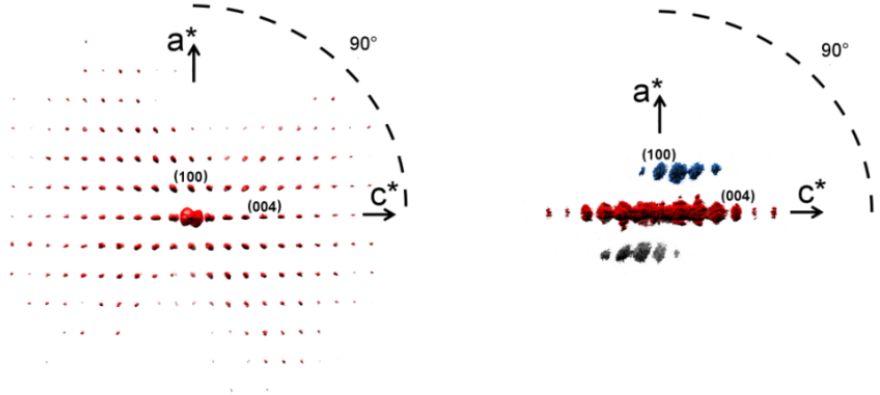

Figure S7. Three-dimensional reciprocal volume reconstruction. (right) Projection of experimental 3D data set along [010] and (left) projection of simulated 3D data set along [010] of an ideal hcp lattice (space group: $P6_3/mmc$).

4. Defects in Pd nanoparticle superlattices

Point defects

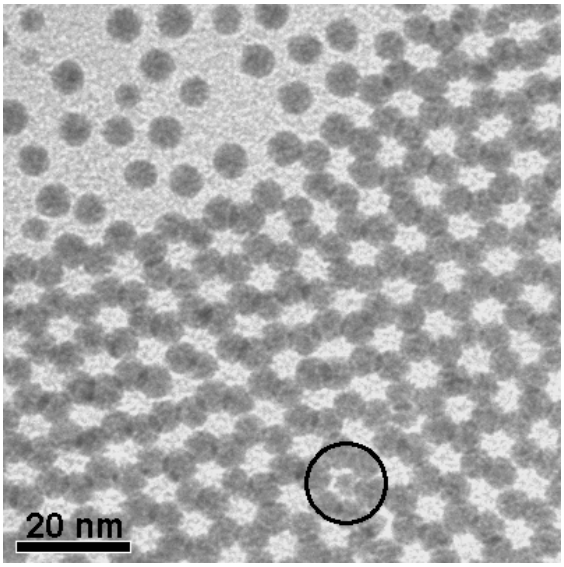

Figure S8. Interstitial defects in a thin nanoparticle array shown inside the black circle.

Planar defects

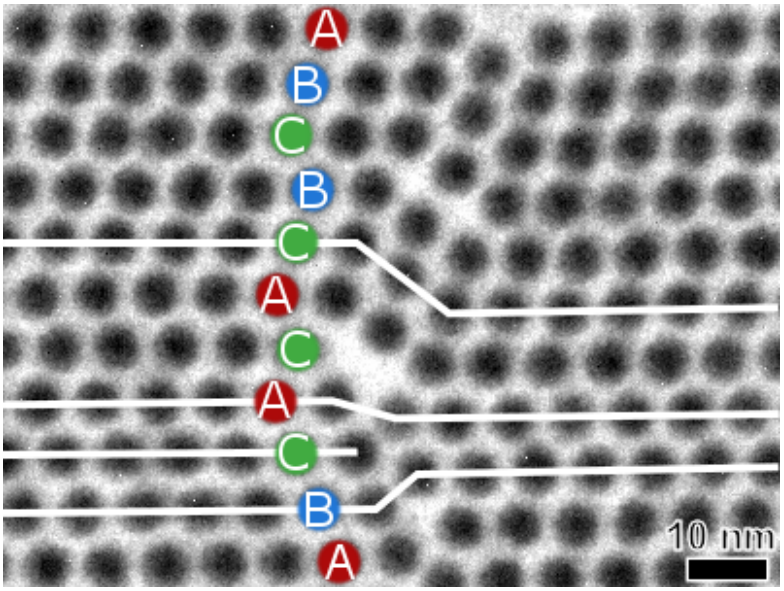

Figure S9. Depiction of two "in plane" stacking faults directions along the $<110>_{fcc}$ planes.

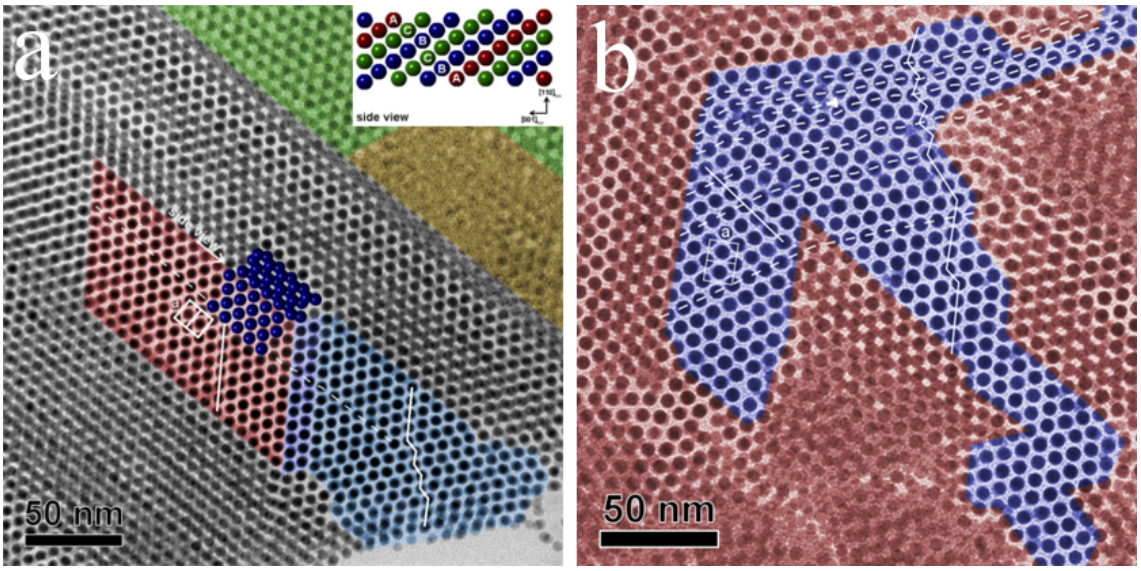

Figure S10. TEM bright-field images revealing highly defected nanoparticle superlattices containing planar defects; (a) in plane (blue area) and out-of-plane (red area) stacking faults along <110>$_{fcc}$ planes; (b) Projection of a complex defected structure showing in-plane stacking faults (red and blue areas) connected to adjacent region of out-of-plane stacking faults. The green area depicts a region of different crystallographic orientation, [111]$_{fcc.}$

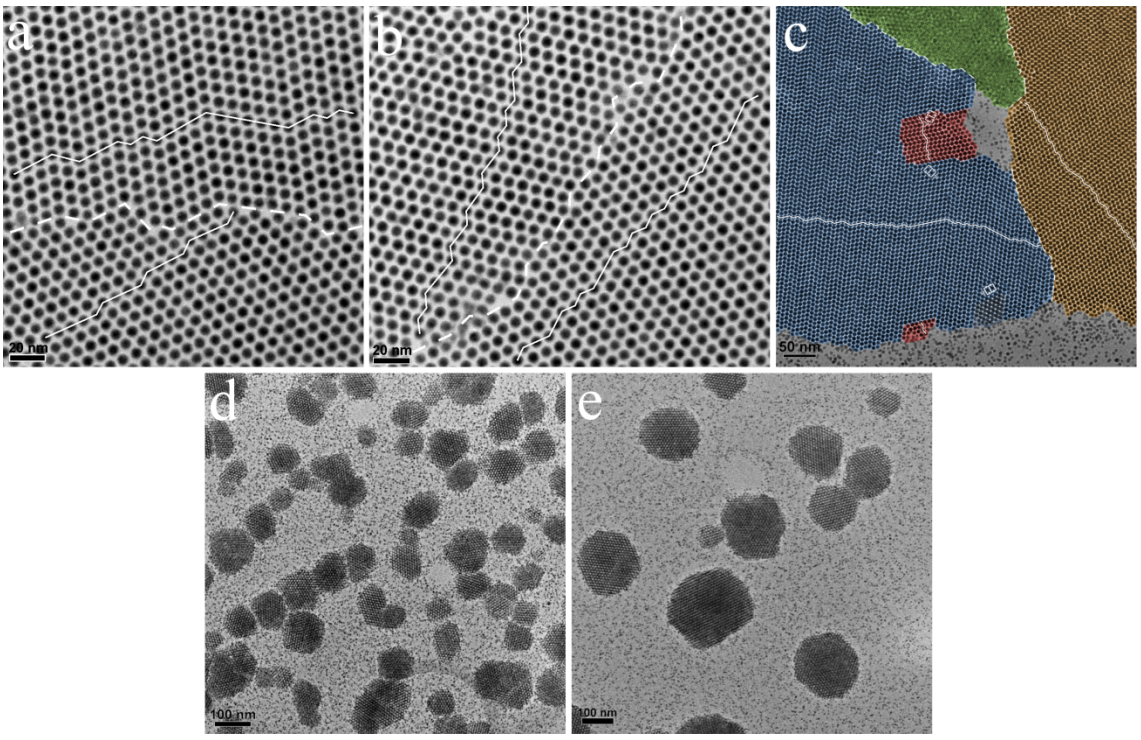

Figure S11. TEM bright-field images depicting planar defects (grain boundaries and stacking faults) in different nanoparticle superlattices. (a,b) The dashed line outlined the grain boundary between two different stacked domains. The traced lines describe the propagation direction of the stacking faults. (c) The different colors define the crystallographic domains of the nanoparticle superlattices. (d-e) Pd nanoparticle superlattices illustrating grain boundaries formation during the assembly process.